AJEMA GLOBAL RESEARCH NETWORK

AMERICAN Journal of Engineering, Mechanics and Architecture
Volume 2, Issue 6, 2024 ISSN (E): 2993-2637

Turbulent Flow Dynamics in A Curved 2D Channel

Abdukhamidov S. K.
Institute of Mechanics and. Seismic stability of structures named after M.T.Urazbaev Academy of Sciences of the Republic of Uzbekistan
Email: Sardor.abdukhamidov@mail.ru

Abstract: This paper investigates the dynamics of turbulent flow in a curved 2D channel, focusing on the changes in flow characteristics due to curvature. Understanding the turbulent flow behavior is crucial for various engineering applications, including pipe design, aerodynamics, and environmental fluid mechanics. The study highlights the effects of centrifugal forces, flow separation, and secondary vortices that develop due to the curvature. Numerical simulations are performed using Reynolds-Averaged Navier-Stokes (RANS) equations with appropriate turbulence models. Results show that flow separation occurs on the inner wall of the curved channel, while strong secondary flows arise, significantly influencing the velocity distribution and pressure gradients.

Keywords: Turbulent Flow, Curved Channel, 2D Flow Dynamics, Centrifugal Forces, Flow Separation, Secondary Vortices, RANS Simulation.

1. Introduction

Turbulent flows in curved channels present unique characteristics compared to flows in straight channels due to the influence of centrifugal forces. These forces result from the curvature and generate secondary motions that strongly affect the overall flow dynamics. Understanding these dynamics is essential in many engineering systems, including piping networks, heat exchangers, and open channel flows. In particular, the generation of secondary vortices due to curvature can lead to increased energy dissipation and affect the structural integrity of engineering designs [1].

Curved channels introduce complex interactions between inertial forces and pressure gradients, resulting in flow separation, recirculation, and secondary circulation patterns. These phenomena are governed by the Reynolds number, channel geometry, and turbulence characteristics. In this study, we focus on the behavior of turbulent flow in a curved 2D channel, using numerical simulations to explore the effects of channel curvature on flow velocity, pressure distribution, and turbulence structures [2], [3], [4], [5].

2. Methodology

The numerical simulations are conducted using the Reynolds-Averaged Navier-Stokes (RANS) equations. The k-epsilon turbulence model is chosen for its balance between computational efficiency and accuracy in predicting turbulent flow behavior. The 2D curved channel is modeled with a fixed curvature radius, and inflow boundary conditions are set to maintain a fully developed turbulent flow at the inlet. The simulations are performed for varying Reynolds numbers to capture the transition and changes in flow behavior [6].

The computational grid is refined near the channel walls to accurately capture boundary layer effects and flow separation zones. Post-processing of the results includes analyzing velocity profiles, pressure distributions, and the development of secondary vortices [7].

The boundary layer is a thin layer of fluid that forms on the surface of an object moving relative to fluid. The study of boundary layers is important in many engineering applications, including aerodynamics and fluid mechanics. The main purpose of this test is the implementation of the two-fluid turbulence model in *Comsol Multiphysics* and compare the obtained results with the experimental data presented on the NASA website for turbulent flow in a curved flat channel. Experimental data were obtained in [8]. The experiment uses a rectangular air duct of constant area with a height of 0.127 m with a quick bend of 30 degrees (internal radius of curvature is 0.127 m) Fig. 4. In the experiment, the aspect ratio of the duct was 6:1. This case represents a flow in a channel with Mach number M = 0.093 and Reynolds number Re = 2,100,000.

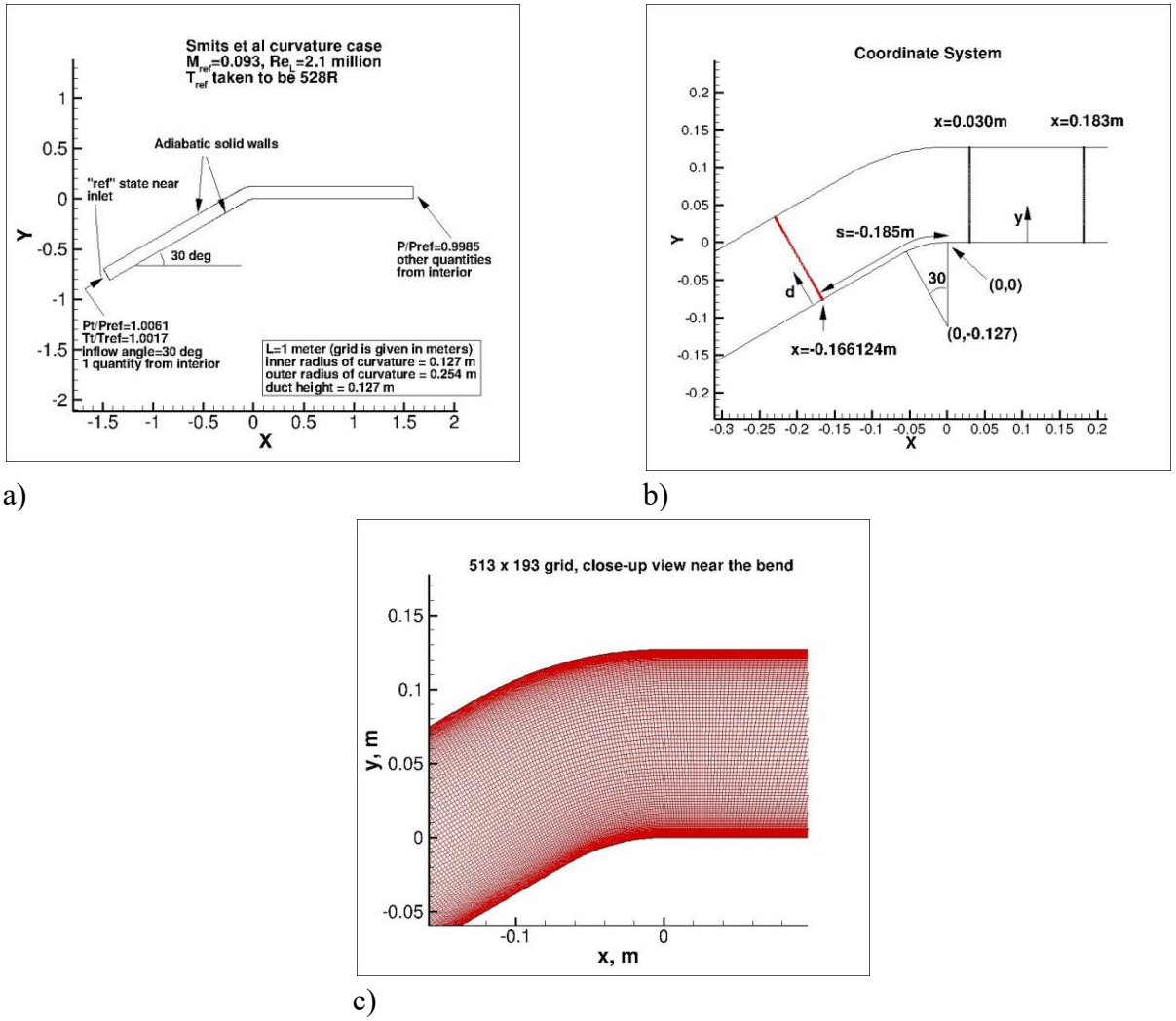

Figure 1. Curved channel. a) boundary conditions c) coordinate frame and b) calculation grid.

In Fig. 4 (U_{ref}) the average velocity near the entrance is 31.9 m/s. P_t is the total pressure, P is the static pressure, and T_t is the total temperature. The distance to the upstream inlet is chosen so as to allow for the natural development of a fully turbulent boundary layer and to provide approximately the correct thickness of the boundary layer before the bend. The upper and lower boundaries are modeled by adiabatic solid walls. A computational grid of 513 × 193 was used, which is presented on the NASA website [9], [10], [11].

The distribution of the surface pressure coefficient on the channel wall is characterized by a change in pressure on its surface depending on the distance from a certain point. Generally, the analysis uses the surface pressure coefficient C_p, defined as the ratio of the pressure difference between a point on the surface of the profile and the pressure of the free flow to the dynamic pressure of the free flow.

$$C_p = \frac{p - p_\infty}{0.5\rho U_0^2},$$

where p is the pressure at a point on the profile surface, P_∞ is the pressure of the free flow, ρ is the density of the free flow, U_0 is the velocity of the free flow.

The coefficient of skin friction C_f is defined as the ratio of the friction force acting on the surface of the profile to the dynamic pressure of the free flow:

$$C_f = \frac{F}{0.5\rho U_0^2 S},$$

where F is the friction force acting on the profile surface, S is the profile surface area oriented along the flow.

Below comparisons of the obtained numerical results with known experimental data are given. Figure 5 shows: a) the dependence of the friction coefficient on pressure; b) the friction coefficient of the lower part of the channel; and c) the friction coefficient of the upper part of the channel, and the results of the experiment [12].

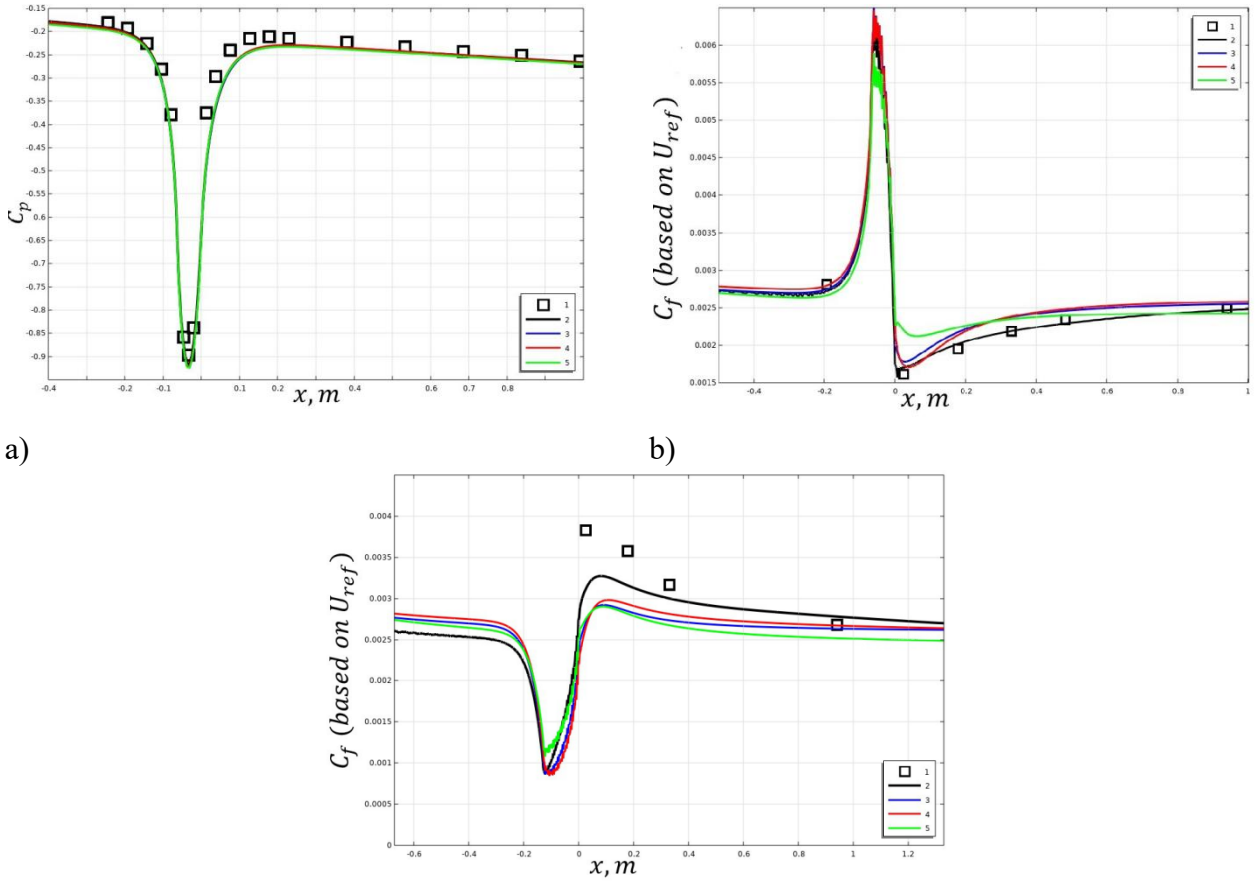

a) b)

c)

Figure 2. 1-experiment, 2-two-fluid model, 3-SST model, 4-SA model, 5-v2-f model.

Figure 5 a) shows that the results of the pressure coefficient for all models are in good agreement with the experiment. For the friction coefficient on the lower surface of the channel 5 b), the two-fluid model shows good results, while the other models show somewhat worse results. For the friction coefficient on the upper surface, the results of all models deviate noticeably from the experimental data. However, the closest results to the experimental data are observed for the two-fluid model [13-15].

Figure 6 shows the profiles of the longitudinal velocity U (m/s) along the lower surface of the channel at different sections downstream.

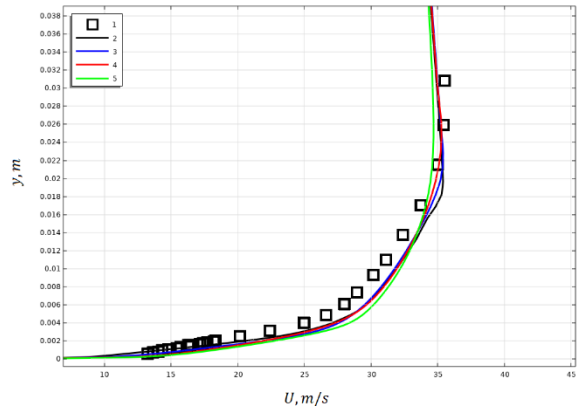

a)

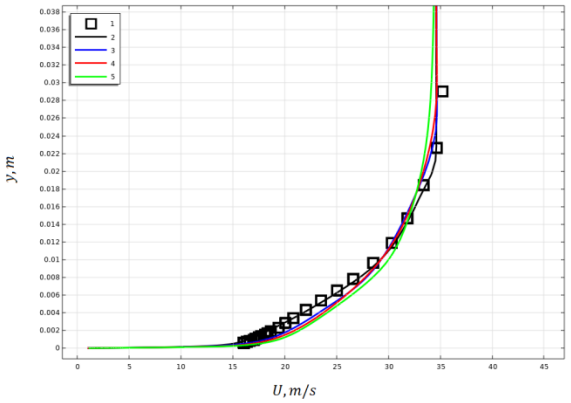

b)

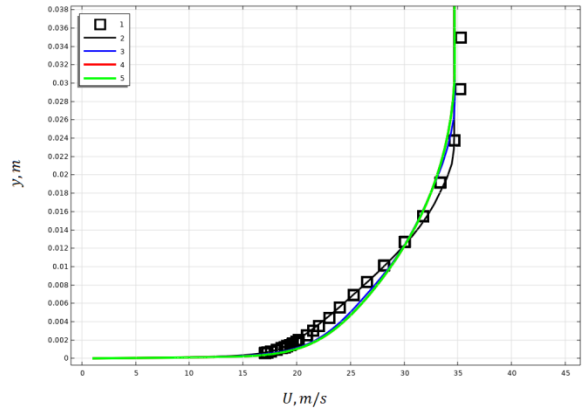

c)

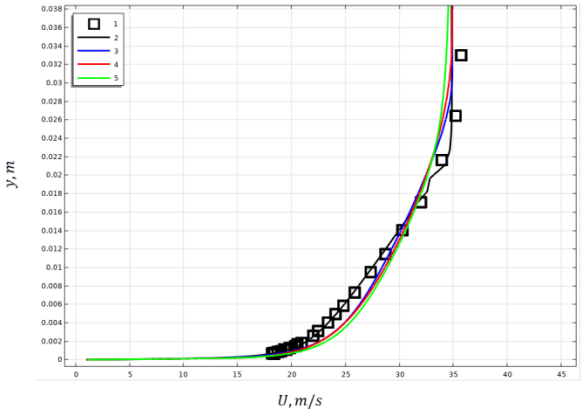

d)

Figure 3. Longitudinal velocity profiles on the lower surface at x = 0.03 a), 0.183 b), 0.335 c), 0.635 d) 1-experiment, 2-two-fluid model, 3-SST model, 4-SA model, 5-v2 -f model.

As seen from Fig. 6, the results of the two-fluid model are close to the results of the experiment. The results of other turbulence models deviate from experimental data at large distances from the bend.

Figure 7 shows the numerical results of turbulence models and experiments for turbulent stress $\overline{u'\vartheta'}$ profiles at cross-sections x=0.03, 0.183, 0.335, 0.635.

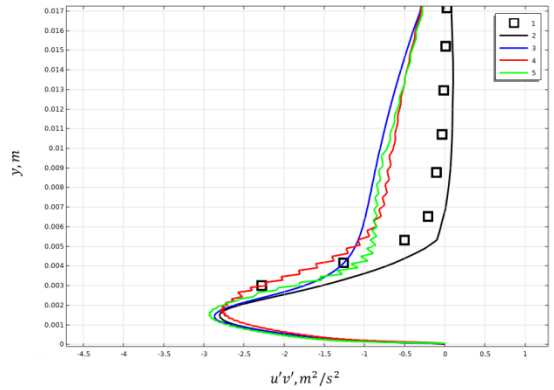

a)

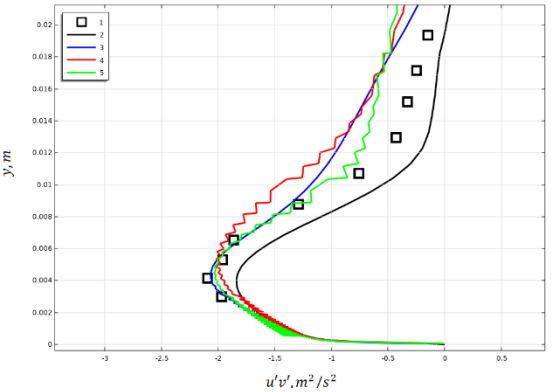

b)

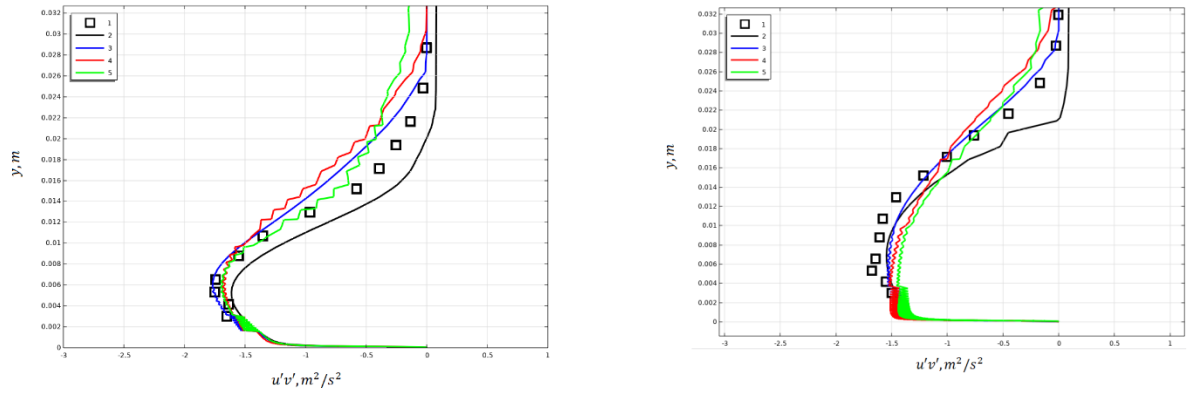

c) d)

Figure 4. Profiles of turbulent stresses on the lower surfaces at x = 0.03 a), 0.183 b), 0.335 c), 0.635 d) 1-experiment, 2-two-fluid model, 3-SST model, 4-SA model, 5-v2- f model.

The two-fluid model makes it possible to obtain all turbulent stresses. Therefore, Figure 8 shows the numerical results of the two-fluid model for turbulent stress profiles $\overline{u'u'}$ and $\overline{v'v'}$ in sections x=0.03, 0.183, 0.335, 0.635 [16], [17], [18].

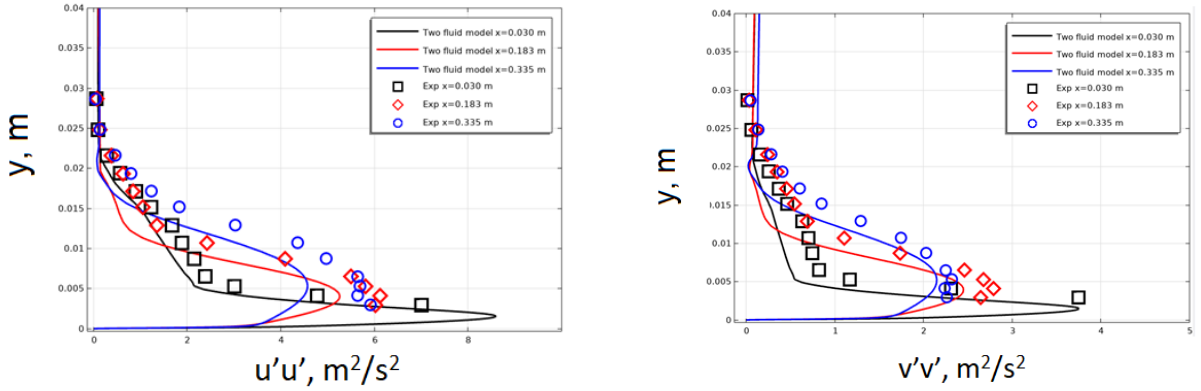

a) b)

Figure 5. Profiles of turbulent stresses on the lower surfaces at a) $\overline{u'u'}$ and b) $\overline{v'v'}$.

Figure 9 shows the isolines of the longitudinal, transverse velocity, pressure, and turbulent stresses according to the two-fluid model in the concave part of the channel.

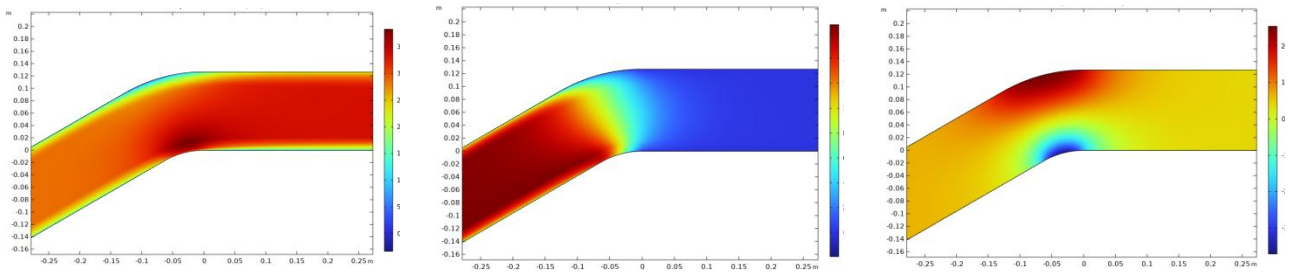

a) b) c)

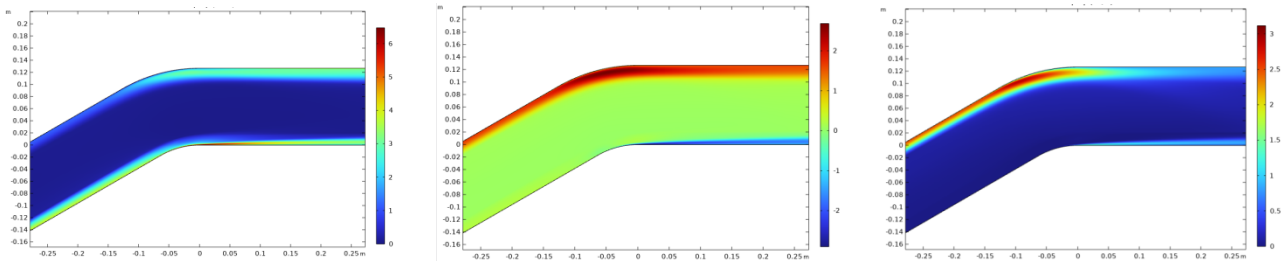

d) e) f)

Figure 6. Isolines a) longitudinal velocity –U, b) transverse velocity –V, c) pressure–p , turbulent stresses d) $\overline{u'v'}$, e) $\overline{u'u'}$, f) $\overline{v'v'}$ concave part of the channel.

It is known that near convex walls the levels of turbulence decrease in comparison with the flow near straight walls. Here, the turbulence model can be evaluated for its ability to capture this effect. We can say that the two-fluid model reflects this situation very well [19].

3. Results and discussions

The results of the numerical simulations reveal several critical aspects of turbulent flow in curved channels:

Flow Separation: The curvature of the channel induces a centrifugal force that pushes the fluid outward, leading to a pressure gradient that causes flow separation near the inner wall. This separation creates a recirculation zone, reducing the effective flow area and increasing local turbulence intensity.

Secondary Flow Development: The secondary vortices, which arise due to the curvature, are observed in the cross-sectional plane of the channel. These vortices significantly influence the velocity profile, leading to a skewed distribution with higher velocities near the outer wall [20].

Pressure Distribution: The pressure distribution along the curved channel exhibits a significant drop in pressure near the outer wall, where the fluid accelerates due to the centrifugal forces. In contrast, the inner wall experiences a higher pressure region, correlating with the flow separation and recirculation.

Turbulent Kinetic Energy: The turbulent kinetic energy is found to be higher near the outer wall, where the velocity gradients are most pronounced due to the combined effects of curvature and flow acceleration.

The study also demonstrates that as the Reynolds number increases, the intensity of the secondary flows and the extent of flow separation grow, further influencing the turbulent structures within the channel. The interaction between the primary flow and secondary vortices leads to complex mixing patterns, which are critical for applications such as heat transfer and pollutant dispersion [21], [22].

4. Conclusion

The turbulent flow in a curved 2D channel exhibits distinctive characteristics compared to straight channels, primarily due to the influence of centrifugal forces and the resulting secondary motions. Flow separation near the inner wall and the development of secondary vortices near the outer wall are key features that must be considered in the design of curved flow systems. Numerical simulations using RANS equations and the k-epsilon turbulence model provide insights into the velocity, pressure, and turbulence structures that arise in these flows. These findings have implications for engineering applications in fluid transport, energy systems, and environmental flows, where curved channels are commonly used.

References

[1]. W. Orozco Murillo, J. A. Palacio-Fernandez, I. D. Patiño Arcila, J. S. Zapata Monsalve, and J. A. Hincapié Isaza, "Analysis of a jet pump performance under different primary nozzle positions and inlet pressures using two approaches: One dimensional analytical model and three dimensional CFD simulations," Journal of Applied and Computational Mechanics, vol. 6, no. Special Issue, pp. 1228–1244, 2020.

[2]. A. S. Kozelkov and V. V. Kurulin, "Eddy-resolving numerical scheme for simulation of turbulent incompressible flows," Computational Mathematics and Mathematical Physics, vol. 55, pp. 1232–1241, 2015.

[3]. K. N. Volkov, V. N. Emel'yanov, and A. G. Karpenko, "Preconditioning of Navier–Stokes equations in the computation of free convective flows," Computational Mathematics and Mathematical Physics, vol. 55, pp. 2080–2093, 2015.

[4]. A. V. Babakov, "Program package FLUX for the simulation of fundamental and applied problems of fluid dynamics," Computational Mathematics and Mathematical Physics, vol. 56, pp. 1151–1161, 2016.

[5]. P. R. Spalart and V. Venkatakrishnan, "On the role and challenges of CFD in the aerospace industry," Aeronautical Journal, vol. 120, no. 1223, pp. 209–232, 2016.

[6]. A. S. Kozelkov, O. G. Krutyakova, V. V. Kurulin, S. V. Lashkin, and E. S. Tyatyushkina, "Application of numerical schemes with singling out the boundary layer for the computation of turbulent flows using eddy-resolving approaches on unstructured grids," Computational Mathematics and Mathematical Physics, vol. 57, pp. 1036–1047, 2017.

[7]. J. Boussinesq, Essai sur la théorie des eaux courantes. Paris, France: Académie des Sciences, 1877.

[8]. A. N. Kolmogorov, "Dissipation of energy in locally isotropic turbulence," Doklady Akademii Nauk SSSR, vol. 30, no. 4, pp. 299–303, 1941.

[9]. L. Prandtl, "Untersuchungen zur ausgebildeten Turbulenz," Zeitschrift für Angewandte Mathematik und Mechanik, vol. 5, 1925.

[10]. T. von Kármán, "Mechanische Ähnlichkeit und Turbulenz," Nachrichten von der Gesellschaft der Wissenschaften zu Göttingen, 1930.

[11]. NASA Langley Research Center, "Turbulence modeling resource." [Online]. Available: http://turbmodels.larc.nasa.gov

[12]. P. R. Spalart and S. R. Allmaras, "A one-equation turbulence model for aerodynamic flows," in AIAA Paper 1992-0439, 1992.

[13]. F. R. Menter, "Zonal two-equation k-ω turbulence models for aerodynamic flows," in AIAA Paper 1993-2906, 1993.

[14]. F. R. Menter, M. Kuntz, and R. Langtry, "Ten years of industrial experience with the SST turbulence model," in Turbulence, Heat and Mass Transfer 4. Begell House, 2003, pp. 625–632.

[15]. A. A. Pasha, "Study of parameters affecting separation bubble size in high speed flows using k-ω turbulence model," Journal of Applied and Computational Mechanics, vol. 4, no. 2, pp. 95–104, 2018.

[16]. P. R. Spalart and M. L. Shur, "On the sensitization of turbulence models to rotational and curvature," Aerospace Science and Technology, vol. 1, no. 5, pp. 297–302, 1997.

[17]. J. Slotnick et al., "CFD Vision 2030 study: A path to revolutionary computational aerosciences," NASA CR-2014-21878, 2014. [Online]. Available: http://ntrs.nasa.gov/search.jsp?R=20140003093

[18]. A. Abbas-Bayoumi and K. Becker, “An industrial view on numerical simulation for aircraft aerodynamic design,” Journal of Mathematics in Industry, vol. 1, no. 1, 2011.
[19]. P. R. Spalart, W. H. Jou, M. Strelets, and S. R. Allmaras, “Comments on the feasibility of LES for wings and on a hybrid, RANS/LES approach,” in Advances in DNS/LES, 1997, pp. 137–147.
[20]. Z. Malikov, “Mathematical model of turbulence based on the dynamics of two fluids,” Applied Mathematical Modelling, vol. 82, pp. 409–436, 2020.
[21]. Z. M. Malikov and M. E. Madaliev, “Numerical simulation of separated flow past a square cylinder based on a two-fluid turbulence model,” Journal of Wind Engineering and Industrial Aerodynamics, vol. 231, p. 105171, 2022.
[22]. M. S. Arif et al., “Laminar flow analysis of NACA 4412 airfoil through ANSYS Fluent,” 2022.